

Mg₂Ni alloy for metal hydride electrodes

J. CHEN, D. H. BRADHURST, S. X. DOU, H. K. LIU

*Institute for Superconducting & Electronic Materials, University of Wollongong,
Northfields Avenue, Wollongong, NSW 2522, Australia
E-mail: shi_dou@uow.edu.au*

A study was made of the effects of ball-milling Mg₂Ni alloy with nickel powder, and chemically coating it with nickel on the alloy properties. Three types of alloys, nickel mixed, nickel ball-milled and nickel coated Mg₂Ni alloy, were used as the active material of metal hydride electrodes. The ball-milling of the alloy with nickel powder results in an amorphous or nanocrystalline phase. Chemical coating of the alloy with nickel was carried out at 25 °C. The alloy particles were pulverised by the colliding process during the ball-milling and possibly by a hydrogen decrepitation mechanism during the coating process. Electrochemical measurements show that the electrode fabricated from the nickel mixed Mg₂Ni alloy was very difficult to charge and discharge at room temperature, while the characteristics of the electrode prepared by nickel ball-milling or nickel coating were greatly improved because of the changed phase structure and surface behaviour. © 1998 Kluwer Academic Publishers

1. Introduction

Nickel–metal hydride (Ni–MH) batteries using hydrogen storage alloys as the negative electrode materials have attracted attention because they are more environmentally acceptable than nickel–cadmium batteries, and also have higher energy density and higher charge rate capability [1–3]. Of all the hydrogen storage alloys studied previously [4], MmNi₅ system alloys (Mm is mischmetal), or zirconium-based Laves phase alloys are normally used as the active material of metal hydride electrodes in Ni–MH batteries [5, 6]. The discharge capacity for MmNi₅ system alloy electrodes has approached the theoretical capacity limit (372 mAh g⁻¹). The activation and electrocatalytic activity for the zirconium-based Laves phase alloy electrode is still inferior to the MmNi₅ system alloy. The Mg-based hydrogen storage alloy is considered as a promising candidate for increasing the capacity of metal hydride electrodes because this alloy is superior to the MmNi₅ system and the Zr-based Laves phase alloy in theoretical hydrogen absorption capacity and material cost [7]. It is known that conventional Mg₂Ni alloy absorbs hydrogen readily at high temperatures under high pressure [8]. Recently, the charge–discharge properties of Mg-based alloy at room temperature have been improved greatly by some research groups [9–12]. In particular, the partial substitution of Mg by Al from Mg₂Ni and the ball-milling of Mg₂Ni alloy with graphite or Ni powder were found to be very useful methods for improving the high discharge capacity. However, the capacity decay was still serious, which made it difficult for these alloys to be used as the active material of a metal hydride electrode. The chemical coating of hydrogen storage alloys with a thin layer of electroless-plated metal such as Cu or Ni has been found to be an effective way to improve the alloy

performance [13, 14]. In view of the reactive nature of magnesium-based alloy in alkaline electrolyte, nickel was chosen for coating the surface of Mg₂Ni alloy powder. A comparison was made between the coated alloy and a Mg₂Ni alloy ball-milled with Ni powder to investigate the effects on the discharge capacity and cycle life of the electrodes.

2. Experimental details

The Mg₂Ni alloy was prepared according to the following powder metallurgical sintering technique. The appropriate amounts of Mg and Ni powders ($\leq 3 \mu\text{m}$ from Aldrich Chemical Company) with the purity of at least 99.7 wt% were thoroughly mixed and pressed into pellets. The pellets were first sintered at 600 °C for 10 h under an argon atmosphere, then ball-milled into powders which were sieved to control the particle size in the range between 36 to 46 μm . The ball-milled alloy was prepared by mixing the above alloy with 10 wt% nickel powder, and ball-milling with stainless steel balls in a stainless steel vessel under the protection of argon atmosphere by using Fritsch planetary high energy equipment at a speed of 160 r.p.m for 10 h. The nickel-coated alloy was prepared by chemical coating with 10 wt% Ni at 25 °C using the solution listed in Table I. Structure and phase identification of the alloy powders were confirmed by X-ray diffraction (XRD) using a Philips PW 1010 diffractometer with CuK α radiation. The surface morphology was examined using a Leica/Cambridge Stereoscan 440 scanning electron microscope (SEM) equipped with energy dispersive spectroscopy (EDS). Particle size distribution and specific surface area of the nickel-mixed, nickel-ball-milled, and nickel-coated alloys were examined using a Malvern particle analyser (PA).

TABLE I Basic composition and operating conditions of the solution for nickel coating of Mg₂Ni alloy

Component	Concentration (mol dm ⁻³)
NiSO ₄ ·6H ₂ O	0.28 to 0.34
Na ₃ C ₆ H ₅ O ₇ ·2H ₂ O	0.5
NH ₄ Cl	0.25
NaH ₂ PO ₂ ·H ₂ O	0.5
Thiourea	0.004 g dm ⁻³
Rotation speed	150 r.p.m.
Temperature	25 °C
pH	8 to 8.5

For comparison, three types of electrodes, the mixture of the Mg₂Ni alloy with 10 wt % nickel powder (A), the 10 wt % nickel ball-milled alloy (B) and the 10 wt % nickel coated alloy (C), were prepared by intimately mixing the A, B or C powders with 1 wt % polytetrafluoroethylene (PTFE) binder and pressing on both sides of a nickel mesh to form a sandwich type structure with a surface area of 1 cm².

The electrochemical cell consisted of the MH working electrode, the NiOOH/Ni(OH)₂ counter electrode, and a Hg/HgO reference electrode. The electrolyte was 6 M KOH solution and the temperature was controlled at 25 °C. Electrode properties were measured by use of an automatic galvanostatic charge/discharge unit interfaced with a Macintosh Performa 6300 computer and a MacLab with Chart 3.3 software. The electrodes were charged at 50 mA g⁻¹ for 20 h, rested for half an hour and then discharged at 50 mA g⁻¹ to -600 mV versus the Hg/HgO electrode. The discharge capacity of each electrode was expressed in mAh per gram of the alloy. When the capacity was calculated, only the weight of the hydrogen storage alloy was considered. Anodic potentiostatic polarization (APP) curves were obtained using an AMEL model 553 potentiostat. The electrochemical impedance spectroscopy (EIS) experiments were performed at 25 °C using an EG&G Princeton Applied Research model 6310. The impedance data were collected as a function of frequency scanned from the highest (10 kHz) to the lowest value (5 mHz). The impedance data were analysed with the aid of a CNLS fitting program, enabling the contact and the charge-transfer resistances to be separated.

3. Results and discussion

Discharge curves of the A, B and C electrodes at a current density of 50 mA g⁻¹ in the first cycle are shown in Fig. 1. It can be clearly seen that the discharge performance of the Mg₂Ni alloy electrode is greatly improved by the ball-milling and nickel-coating. No discharge plateau was detected for the A electrode, but a plateau of discharge potential was observed at -0.83 V versus Hg/HgO electrode for the B and C electrodes. Discharge capacities for the A, B and C electrodes were 95, 680, and 756 mAh g⁻¹, respectively. These results show that the nickel ball-milling and nickel coating of Mg₂N alloy are very effective methods of increasing the discharge capacity of the alloy electrode.

TABLE II Discharge capacity of A, B and C electrodes at different discharge current density

Discharge current density (mA g ⁻¹)	Capacity (mAh g ⁻¹)		
	A	B	C
50	95	680	756
100	5	538	612
200		390	440

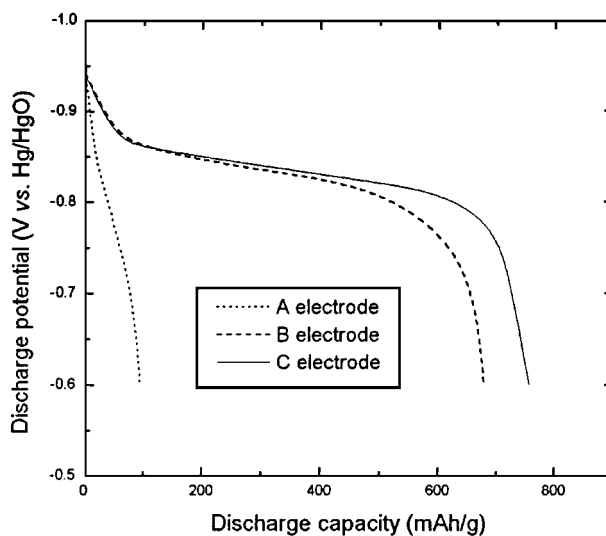


Figure 1 Discharge curves (the first cycle) of the nickel mixed, nickel ball-milled, and nickel coated Mg₂Ni alloy electrodes.

The discharge capacities of the A, B and C electrodes at different discharge current densities are given in Table II. It is obvious that the high-rate discharge capability of the Mg₂Ni alloy electrode was greatly improved by the nickel ball-milling and nickel coating. The discharge capacities of the A electrode at 50 mA g⁻¹ and at 100 mA g⁻¹ were 95 mAh g⁻¹ and 5 mAh g⁻¹, respectively. However, the discharge capacity obtained at a discharge current density of 100 mA g⁻¹ was 538 mAh g⁻¹ for the B electrode and 612 mAh g⁻¹ for the C electrode, approximately 78 and 81% of that obtained at 50 mA g⁻¹, respectively. Moreover, values of 390 mAh g⁻¹ for the B electrode and 440 mAh g⁻¹ for the C electrode were obtained at the relatively high discharge current density of 200 mA g⁻¹.

In order to find out the reasons responsible for the great increase of discharge capacity and improvement of high rate discharge of the Mg₂Ni alloy after ball-milling with nickel or chemical coating with nickel, two aspects, alloy phase and surface properties were analysed by XRD, SEM, PA, and electrochemical methods such as APP and EIS.

The A, B and C alloy powders were analysed by XRD, as shown in Fig. 2. It can be seen that the X-ray pattern of the A alloy powder shows the presence of the hexagonal phase for Mg₂Ni and pure nickel. It is interesting that the X-ray patterns of the B and C alloy powders have been changed. For alloy B, the characteristic peaks of the Mg₂Ni alloy phase decreased in intensity and broadened. This result indicates that

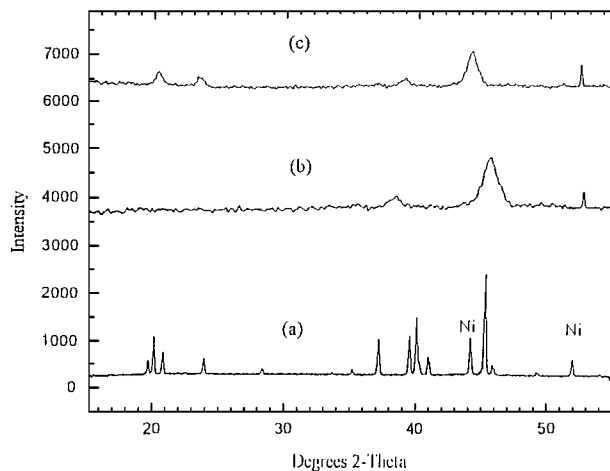


Figure 2 XRD patterns for the nickel mixed (a), nickel ball-milled (b), and nickel-coated (c) Mg_2Ni alloy.

there was a phase transformation from polycrystalline to amorphous or nanocrystalline state. For alloy C, the characteristic peaks of Mg_2Ni alloy phase broadened and shifted to lower angles, which might indicate that an absorption of hydrogen into alloy had occurred due to the hydrogen produced in the chemical process.

The surface morphology of the A, B and C alloy powders are shown in Fig. 3. It is clear that the surface of alloy A is smooth, but the surface of alloy B appears honeycombed, while that of alloy C is rough and protruding. The honeycombed and protruding areas visible in Fig. 3b and c were analysed by EDS. It was found that one of the honeycombed areas contained Mg and Ni in the atomic ratio of Mg : Ni = 2.0 : 1.2, which is lower than that of the alloy Mg_2Ni (Mg : Ni = 2.0 : 1.0). This indicates a high degree of dispersion of nickel in the alloy to form a non-stoichiometric structure. For the protruding areas in Fig. 3c, only nickel was found, and this shows that the chemical coating on the Mg_2Ni alloy surface was relatively pure nickel.

Particle size distributions and specific surface areas of the A, B and C alloy powders are given in Table III. Since the particle size and specific surface area measured contains the quantity of the added nickel powder, each value in Table II (for A and B) was obtained by subtracting that of nickel powder. It can be shown that the ball-milling and nickel coating processes result in a gradual reduction in the lamella spacing from 36–45 μm for the A alloy powder to 5–10 μm and 18–25 μm for the B and C alloy powders, respectively. Also it is obvious that the B alloy powder has the largest specific surface area, while the A alloy powder has the smallest one. Although both the ball-milling and nickel coating processes result in particle pulveri-

TABLE III Particle size distribution (PSD) and specific surface area (SSA) of the nickel mixed, nickel ball-milled and nickel coated alloys

Sample	PSD (μm)	SSA ($m^2 g^{-1}$)
A	36–45 (90%)	0.22
B	5–10 (91%)	0.98
C	18–24 (93%)	0.56

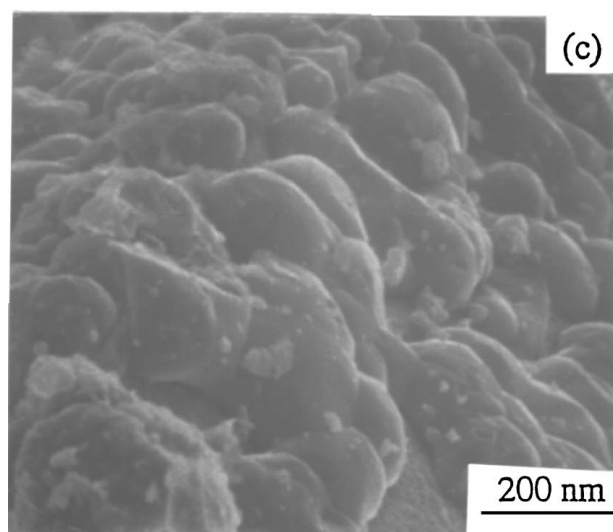
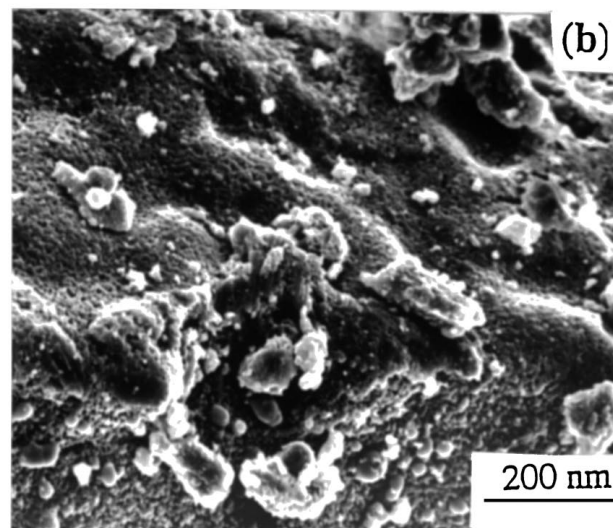
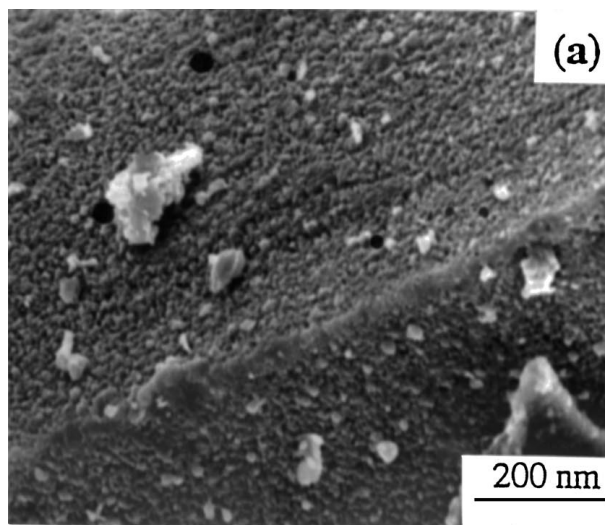


Figure 3 SEM images for the nickel mixed (a), nickel ball-milled (b), and nickel-coated (c) Mg_2Ni alloy.

sation and increase of the specific surface area, they are achieved in different ways. For the ball-milling of the alloy with nickel powder, it is by means of prolonged time colliding between the balls and the alloy particles. Subsequently the alloy particles are fractured

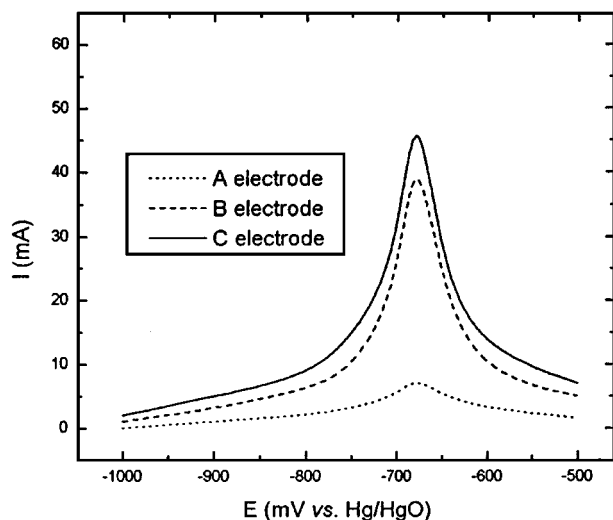
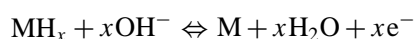


Figure 4 Anodic potentiostatic polarization curves for the electrodes of the nickel mixed, nickel ball-milled and nickel-coated Mg_2Ni alloy.

and interdiffusion takes place resulting in the large increase of specific surface area observed. In the case of the chemical coating process, it is possible that the alloy pulverisation is caused by a decrepitation mechanism due to hydrogen penetration during the coating because of the high concentration of the reducing agent hypophosphite.

The A, B and C alloy electrodes were selected to further investigate the electrode kinetics of the hydriding/dehydriding reactions. Fig. 4 shows the potentiostatic polarization curves for these electrodes after fully charging at the first cycle. The anodic peak current at -680 mV versus Hg/HgO was attributed to the oxidation of hydrogen absorbed in the alloy according to the equation



It can be seen that the anodic peak current of hydrogen oxidation varies with the different electrodes, and is much more prominent for the B and C alloy electrodes than for the A alloy electrode. The higher the anodic peak current, the larger the catalytic activity for hydrogen oxidation of the electrode.

Table IV summarizes the EIS results for the A, B and C alloy electrodes. The contact resistance and charge-transfer resistance were at their maximum values for the A alloy electrode. This may be the reason why it was difficult to charge and discharge. Similar contact resistance and charge-transfer resistance values were found for the B and C alloy electrodes. These were also much lower than those of the A alloy electrode. The decreased

TABLE IV Contact resistance (R_{CR}) and charge-transfer resistance (R_{CTR}) of the A, B and C alloy electrodes

Alloy	R_{CR} (Ω)	R_{CTR} (Ω)
A	0.28	2.52
B	0.14	0.68
C	0.12	0.66

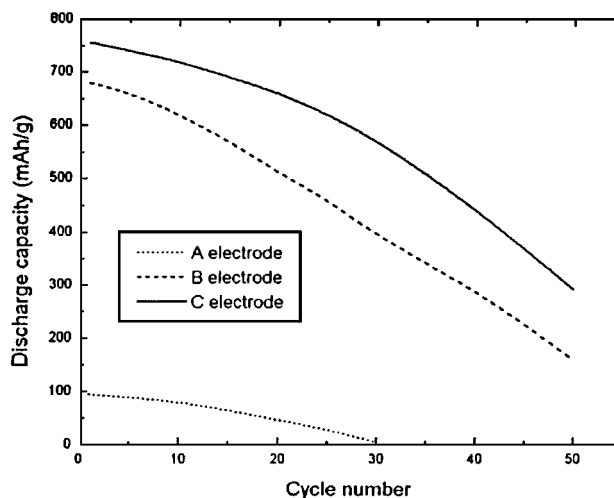


Figure 5 Discharge capacities of the nickel mixed, nickel ball-milled, and nickel coated Mg_2Ni alloy electrodes as a function of cycle number.

contact and charge-transfer resistances could reduce the overpotential of the charge/discharge processes and increase the hydrogen diffusion in the alloy electrodes. As a result, the discharge capacity would be increased and the high rate discharge capability improved for the nickel ball-milled and nickel coated alloy electrodes.

Discharge capacities of the A, B and C alloy electrodes as a function of cycle number are shown in Fig. 5. The initial discharge capacity of the electrode was markedly increased from 95 mAh g^{-1} for the A alloy electrode to 680 mAh g^{-1} for the B alloy electrode and 756 mAh g^{-1} for the C alloy electrode. The capacity decay of the three kinds of electrodes proceeds very fast. For examples, a discharge capacity of only 5 mAh g^{-1} was measured for the A alloy electrode at the 30th cycle, while the discharge capacity of 160 mAh g^{-1} was found for the B alloy electrode and 290 mAh g^{-1} for the C alloy electrode after 50 charge–discharge cycles.

To analyse the capacity decay of the A, B and C alloy electrodes, the A alloy electrode after 30 cycles and the B, C alloy electrode after 50 cycles were dried in a vacuum over at 70°C for 2 h, and then the active materials from these electrodes were separated from the nickel mesh substrate and ground for XRD analysis. The results are shown in Fig. 6. It can be seen that $Mg(OH)_2$

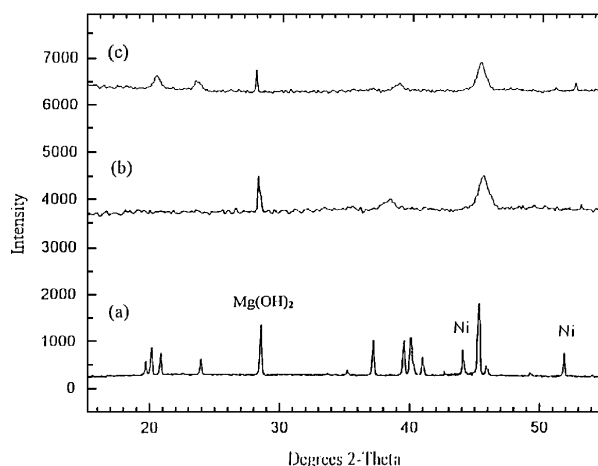


Figure 6 XRD patterns for the nickel mixed (a), nickel ball-milled (b), and nickel-coated (c) Mg_2Ni alloy electrode.

was formed not only in the A alloy but also in the B and C alloys. However, the peak intensity of this oxide is much stronger in alloy A compared with that in alloy B or alloy C. The serious oxidation of the A alloy is because of its more active reaction in the alkaline electrolyte. The oxidation of the B and C alloy electrodes is prevented to an extent because of the protection of the ball-milled or chemically coated nickel layer, but it cannot be completely effective because: (i) the ball-milled or chemically coated nickel on the alloy surface is not homogeneous; and (ii) the alloy is disintegrated during the repeated charging and discharging process which brings about the gradual pulverisation of the alloy, continuously enlarged surface area, and production of fresh surface, resulting in continuous degradation of the alloy.

From all the results above, it has been found that the nickel ball-milling or nickel coating can result in a nickel-rich surface layer, which is thought to prevent the oxidation of the alloy to some extent. The subsurface layer of the ball-milled alloy [15] or the nickel coated alloy is strongly disordered, which is responsible for its apparent transparency to hydrogen. Around the nickel particles there are also nickel atoms or clusters that exhibit increased catalytic activity owing to the electron transfer from Mg to Ni. A subsidiary effect is the increased surface area which enhances the number of sites for redox hydrogen reactions. Finally, the ball-milled and coated nickel plays a role of microcurrent collector when charging and discharging. Therefore, the process of the ball-milling or the nickel coating is not simply a mixture of two metals, but a metastable system with high reactivity due to the large interface between the metals, the presence of defects, the dislocation of nickel in the alloy and the chemical interaction of the compounds. All of these factors are thought to be beneficial to the hydrogen absorption/desorption (charging and discharging of the electrode), resulting in a significant improvement in alloy performance.

4. Conclusions

Electrochemical measurements on three types of Mg₂Ni alloy electrodes have shown that improvements can be made in their performance by ball-milling the alloy with nickel powder or by chemical coating with nickel on the alloy surface. Both the ball-milling and chemical coating processes cause particle pulverization, the increase of the specific surface area, and a nickel rich surface layer. It is found that the ball-milling

or the chemical coating greatly improves the catalytic activity of the alloy electrode, and this results in a large increase in the electrode capacity and high-rate discharge capability but little influence on the cycle life. The discharge capacities of 680 mAh g⁻¹ and 756 mAh g⁻¹ were achieved at a discharge current density of 50 mA g⁻¹ for the nickel ball-milled and nickel-coated alloy electrodes, respectively. This encouraging result suggests that the kinetics of hydrogen absorption/desorption (charge/discharge) for the Mg₂Ni alloy are greatly improved by the ball-milling or chemical coating processes.

Acknowledgement

Financial support by the Department of Employment, Education and Training (DEET) is gratefully acknowledged.

References

1. J. J. G. WILLEMS and K. H. J. BUSCHOW, *J. Less-Common Metals* **129** (1987) 13.
2. T. SAKAI, M. MATSUOKA and C. IWAKURA, "Handbook of physics and chemistry of rare earths," **21** edited by K. A. Gschneidner, Jr and L. Eyring (Elsevier Science BV, Amsterdam, 1995) 133.
3. J. CHEN and Y. S. ZHANG, *Int. J. Hydrogen Energy* **20** (1995) 235.
4. G. I. DOUGLAS and D. O. NORTHWOOD, *J. Mater. Sci.* **18** (1983) 321.
5. J. J. G. WILLEMS, *Philips J. Res.* **39** (1984) 1.
6. S. R. OVSHINSKY, M. A. FETCENKO and J. ROSS, *Science* **260** (1993) 176.
7. C. IWAKURA, S. HAZUI and H. INOUE, *Electrochem. Acta* **41** (1996) 471.
8. J. J. REILLY and R. H. WISWALL Jr, *Inorg. Chem.* **7** (1968) 2254.
9. Y. Q. LEI, Y. M. WU, Q. M. YANG, J. WU and Q. D. WANG, *Z. Phys. Chem.* **183** (1993) 379.
10. N. CUI, B. LUAN, H. K. LIU, H. J. ZHOU and S. X. DOU, *J. Power Sources* **55** (1995) 263.
11. C. IWAKURA, S. NOHARA, H. INOUE and Y. FUKUMOTO, *Chem. Commun.* **15** (1996) 1831.
12. T. KOHNO and M. KANDA, *J. Electrochem. Soc.* **144** (1997) 2384.
13. K. NAITO, T. MATSUNAMI, K. OKUNO, M. MATSUOKA and C. IWAKURA, *J. Appl. Electrochem.* **23** (1993) 1051.
14. T. SAKAI, H. ISHIKAWA, K. OGURO, C. IWAKURA and H. YONEYAMA, *J. Electrochem. Soc.* **134** (1987) 558.
15. A. STEPANOV, E. IVANOV, I. KONSTANCHUK and V. BOLDYERVA, *J. Less-Common Metals* **131** (1987) 89.

Received 19 June
and accepted 21 June